Magnetic Protoneutron Star Winds and r-Process Nucleosynthesis

Todd A. Thompson[1]

Astronomy Department and Theoretical Astrophysics Center, 601 Campbell Hall, The University of California, Berkeley, CA 94720; thomp@astro.berkeley.edu

ABSTRACT

Because of their neutron-richness and association with supernovae, post-explosion protoneutron star winds are thought to be a likely astrophysical site for rapid neutron capture nucleosynthesis (the r-process). However, the most recent models of spherical neutrino-driven protoneutron star winds do not produce robust r-process nucleosynthesis for 'canonical' neutron stars with a gravitational mass of $1.4\,M_\odot$ and coordinate radius of 10 km. These models fail variously; either the flow entropy is too low, the electron fraction is too high, or the dynamical expansion timescale is too long. To date, no models have included the effects of an ordered dipole magnetic field. We show that a strong magnetic field can trap the outflow in the neutrino heating region, thus leading to much higher matter entropy. We estimate both the trapping timescale and the resulting entropy amplification. For sufficiently large energy deposition rates, the trapped matter emerges dynamically from the region of closed magnetic field lines and escapes to infinity. We find that ordered dipoles with surface fields of $\gtrsim 6\times10^{14}$ G increase the asymptotic entropy sufficiently for robust r-process nucleosynthesis.

Subject headings: nuclear reactions, nucleosynthesis, abundances — stars: magnetic fields — stars: winds, outflows — stars: neutron — supernovae: general

1. Introduction

In the r-process, seed nuclei capture neutrons on timescales much shorter than those for β-decay. For sufficiently high neutron-to-seed ratio ($\gtrsim$ 100), nucleosynthesis proceeds to the heaviest nuclei, forming characteristic abundance peaks at A ∼80, 130, and 195 (Burbidge et al. 1957; Cameron 1957). Observational studies of the relative abundance pattern of r-process elements in ultra-metal-poor ([Fe/H]$\lesssim -2.5$) halo stars reveal remarkable concordance with solar r-process abundances for $A \gtrsim 135$ (e.g. Sneden et al. 1996;

[1]Hubble Fellow

Burris et al. 2000). These observations suggest an astrophysical r-process site that consistently produces the same relative abundance in this mass range, at very early times in the chemical enrichment history of the galaxy. Although the governing nuclear physics is fairly well understood, the astrophysical site for the r-process has yet to be established. Because of their intrinsic neutron-richness, the post-explosion outflows expected from protoneutron stars (PNSs) in the seconds after successful supernovae (SNe) are thought to be a likely candidate site for the r-process (Woosley & Hoffman 1992; Woosley et al. 1994; Burrows, Hayes, & Fryxell 1995).

The characteristics of any potential astrophysical r-process environment that determine the resulting nucleosynthesis are the asymptotic entropy ($s_{\rm a}$; units of $k_{\rm B}$ baryon^{-1} throughout), the electron fraction ($Y_e^{\rm a}$), and the dynamical timescale ($\tau_{\rm dyn}$, the density e-folding time at $T = 0.5\,{\rm MeV}$) near the start of the r-process. In general, higher $s_{\rm a}$, lower $Y_e^{\rm a}$, and shorter $\tau_{\rm dyn}$, lead to larger neutron-to-seed ratios and higher maximum A (e.g. Meyer & Brown 1997). In addition to attaining the requisite $s_{\rm a}$, $Y_e^{\rm a}$, and $\tau_{\rm dyn}$, a potential r-process site must produce a sufficient quantity of r-process ejecta ($M_{\rm ej}^{\rm r}$) per event, so that the total galactic r-process budget is accounted for. For example, if all supernovae produce a robust r-process abundance pattern, then the total mass of r-process material that must be produced and ejected per SN is $M_{\rm ej}^{\rm r} \sim 10^{-5} - 10^{-6}\,{\rm M}_\odot$ (Qian 2000).

Recent PNS *wind* models (not *bubble* models, as in Woosley et al. 1994) fail to produce robust r-process nucleosynthesis up to and beyond the 3$^{\rm rd}$ r-process peak for 'canonical' neutron stars with $M = 1.4\,{\rm M}_\odot$ and $R = 10\,{\rm km}$ (Takahashi, Witti, & Janka 1994; Qian & Woosley 1996 (QW); Otsuki et al. 2000; Wanajo et al. 2001; Thompson, Burrows, & Meyer 2001 (TBM); however, see Terasawa et al. 2002). Indeed, given the $Y_e^{\rm a}$ and $\tau_{\rm dyn}$ derived in these models, most efforts fall short of the required $s_{\rm a}$ by a factor of $3 - 5$.

To date, protoneutron star wind models have neglected the effects of an ordered dipole magnetic field. Nagataki & Kohri (2001) considered the effects of rotation and a monopole-like magnetic field on PNS winds in the spirit of Weber & Davis (1967), but were unable to explore field strengths above $\sim 10^{11}\,{\rm G}$ because of the complicated critical point topologies encountered in that steady-state solution. Although QW speculated on the role of magnetic fields in their wind solutions, the effects discussed were not quantified.

Motivated by multi-dimensional studies of solar coronal hole and helmet streamers, as well as by the very high inferred magnetic field strengths of some neutron stars (*magnetars*, Kouveliotou et al. 1999; Duncan & Thompson 1992), we here consider the effects of an ordered dipole magnetic field on PNS winds and the composition of their ejecta. In this preliminary investigation, we show that strong dipole fields can trap and heat matter in regions of closed magnetic field lines and that this matter may be ejected to infinity with significantly amplified entropy. Our estimates indicate that for magnetar-strength initial dipole fields, the entropy increase is sufficient for a robust r-process.

2. Magnetic Protoneutron Star Winds

The comparison germane for assessing the importance of a dipole magnetic field on the wind evolution is the ratio $\beta = P/(B^2/8\pi)$, between the thermal pressure and the magnetic energy density. In Fig. 1 we compare $P(r)$ for two wind models with $R = 10\,\mathrm{km}$, $M = 1.4\,\mathrm{M}_\odot$, and $L_\nu^{\rm tot} = 3.7 \times 10^{51}\,\mathrm{erg\,s^{-1}}$ (labeled, 'High L_ν') and $L_\nu^{\rm tot} = 1.8 \times 10^{50}\,\mathrm{erg\,s^{-1}}$ ('Low L_ν') with $B^2/8\pi$ (dashed lines) for various surface field strengths (B_0). The spherical wind profiles shown here are obtained by solving the equations of steady-state general-relativistic hydrodynamics in a Schwarzschild metric with a general neutrino energy deposition function using a two-point relaxation algorithm on an adaptive radial mesh (as formulated in TBM). In Fig. 1, we take $B(r) = B_0(R_B/r)^3$, where R_B is a reference radius for the magnetic field footpoints. Because of the exponential near-hydrostatic atmosphere, we set $R_B = 11\,\mathrm{km}$. Fig. 1 shows that as the PNS cools and L_ν decays, the dynamics of PNS winds can be dominated by magnetar-strength magnetic fields. For $B_0 < 10^{14}\,\mathrm{G}$, the magnetic field will only dominate the flow at very late times, when both L_ν and the mass outflow rate ($\dot{M}$) are very small. However, for $B_0 = 10^{15}\,\mathrm{G}$, the magnetic field dominates even the High L_ν wind solution for $r < R_\beta \simeq 30\,\mathrm{km}$, where the relationship $\beta(R_\beta) = 1$ defines R_β. For small B_0, such that R_β does not exist, the field is blown into a roughly monopolar configuration and the mass flow proceeds to infinity unencumbered. However, for high B_0, we expect the global configuration to be much like that derived in multi-dimensional studies of solar coronal holes and helmet streamers (e.g. Pneumann & Kopp 1971; Steinolfson, Suess, & Wu 1982; Usmanov et al. 2000; Lionello et al. 2002): open magnetic field lines at the poles and a region of closed magnetic field lines (a *dead zone*, in the spirit of Mestel 1968) at latitudes near the magnetic equator.

In the closed zone the matter is trapped. In the absence of net heating, this configuration might be long-lived. In the context of PNS winds, however, we expect the pressure of the trapped matter to increase as a result of neutrino energy deposition ($\dot{q}$). If P approaches $B^2/8\pi$ in the closed zone, we expect the matter previously trapped to escape dynamically. Thus, given $\beta < 1$ at $r\,(< R_\beta)$ and a local energy deposition rate $\dot{q}\rho$ [$\mathrm{erg\,cm^{-3}\,s^{-1}}$], the amount of time required to increase P to $B^2/8\pi$ is

$$\tau_{\rm trap} \sim [B^2/8\pi - P]/[\dot{q}\rho]. \qquad (1)$$

Hence, the matter in the closed zone is not trapped permanently, but escapes in $\tau_{\rm trap}$ because of neutrino heating. The increase in P of the trapped gas must be attended by an increase in entropy on account of $\dot{q}$. If $\dot{q}$ and T do not change appreciably in $\tau_{\rm trap}$, $s_{\rm a}$ increases by

$$\Delta s \sim \dot{q}\tau_{\rm trap}/T. \tag{2}$$

If the magnetic field is very weak then $\tau_{\rm trap}$ is very short and $\Delta s \sim 0$. At the other extreme, if $\beta \ll 1$, some of the matter in the closed zone may be permanently trapped (barring MHD instabilities, see §4) because as T gets large, neutrino cooling begins to compete with heating and $\dot{q} \to 0$ locally. The neutrino cooling rates are stiff functions of T ($\propto T^6$ and $\propto T^9$ for $e^-p \to n\nu_e$ and $e^+e^- \to \nu\bar{\nu}$, respectively) and for this reason, T, and, hence, P, cannot increase arbitrarily throughout the closed zone. This sets a maximum P increase attainable at any radius. For example, Fig. 2 shows T, s, and ρ (thin solid lines) for the High L_ν model. Also shown are the maximum temperature achievable at any radius ($T^\star$, dotted line) for fixed ρ and the corresponding maximum entropy ($s^\star$, dotted line). The thick solid line shows $[s + \Delta s]$ as computed from eq. (2), for $B_0 = 5 \times 10^{15}$ G. Because $[s + \Delta s]$ is greater than $s^\star$ for $r < R_q$, the material inside R_q is permanently trapped. This defines R_q. Note that in all models $R_q < R_\beta$. Figure 2 shows that although for very high B_0 some material may be permanently trapped, the material exterior to R_q and interior to R_β may escape with significantly enhanced entropy. In this case, near R_q, $s_{\rm a}$ is increased from ~ 80 to ~ 600.

3. Results

Figure 3 shows $s_{\rm a}$ versus $\tau_{\rm dyn}$ for a 10 km 1.4 $M_\odot$ PNS, for many different L_ν. Each point on the thick solid line is a separate spherical steady-state wind model with no magnetic field effects. As L_ν decreases, the curve evolves from low entropy ($\sim$80) and short $\tau_{\rm dyn}$ ($\sim$4 ms) to higher entropy ($\sim$175) and considerably longer $\tau_{\rm dyn}$ ($\sim$170 ms). One can think of this line as the cooling curve of a PNS composed of snapshots. The dashed line shows the analytical results from Hoffman, Woosley, & Qian (1997) for the $s_{\rm a}$ required for 3$^{\rm rd}$-peak r-process nucleosynthesis at fixed $Y_e^{\rm a}$ and $\tau_{\rm dyn}$. Above this line, for $Y_e^{\rm a} = 0.48$, 3$^{\rm rd}$-peak r-process elements can be synthesized. Below it, the neutron-to-seed ratio is too small for the nuclear flow to proceed to $A \sim 195$. One can see clearly that at all $\tau_{\rm dyn}$, $s_{\rm a}$ is too low to produce a robust r-process for the non-magnetic models.

The thin solid lines in Fig. 3 are obtained from the non-magnetic models (thick solid line) by applying the procedure for calculating $\tau_{\rm trap}$ and Δs described in §2 at each L_ν. Lines for surface magnetic field strengths (B_0) of 2, 4, 6, and 8×10^{14} G as well as 1 and 2×10^{15} G are shown. We assume that $\tau_{\rm dyn}$ is the same between magnetic and non-magnetic models. The increase in enthalpy due to trapping and consideration of the Bernoulli integral indicate that this approximation should hold to no better than a factor of $2 - 3$. For a given B_0, we find that if R_β exists then $R_\beta \propto L_\nu^{-0.75}$ and $\tau_{\rm trap} \propto L_\nu^{-2.7}$, to rough approximation. One can see that for $B_0 = 2\times10^{14}$ G R_β does not exist until $\tau_{\rm dyn}\simeq 0.075$ s. Figure 3 shows that the entropy of the flow is profoundly effected by including a strong dipole magnetic field. As long as $Y_e^{\rm a} < 0.5$, with a surface field $\gtrsim 6\times10^{14}$ G, $s_{\rm a}$ may be increased sufficiently for robust, 3$^{\rm rd}$-peak r-process nucleosynthesis.

Because the solution to the wind equations constitutes an eigenvalue problem for the mass outflow rate ($\dot{M}$), we can estimate the amount of r-process material ejected ($M_{\rm ej}^r$) by the magnetic models by assuming $L_\nu \propto t^{-\alpha}$. For a given B_0, $M_{\rm ej}^r$ is then the time integral of $\dot{M}$ above the dashed line in Fig. 3. Taking $\alpha = 0.9$, the entire range of L_ν in Fig. 3 corresponds to ~ 15 s. Given this $L_\nu(t)$, $M_{\rm ej}^r(B_0 = 2\times10^{15}\,{\rm G})/M_{\rm ej}^r(B_0 = 6\times10^{14}\,{\rm G}) \sim 50$. That is, for higher B_0, more r-process material is ejected. Absolute numbers for $M_{\rm ej}^r$ are misleading because $\dot{M}\propto R^{5/3}$ (QW) and we have not included the PNS radial contraction during the early cooling epoch. However, as a first approximation, taking $R = 30$ km initially, with $R\propto t^{-1/3}$ (until R reaches 10 km), with $L_\nu\propto t^{-0.9}$, and conserving magnetic flux so that when $R = 10$ km, $B_0 = 5\times10^{15}$ G, we find that $M_{\rm ej}^r \sim 10^{-4}\,{\rm M}_\odot$. This number is sensitive to R_q, R_β, and the extent in latitude of the closed zone at the PNS surface, but we conclude that although the birth rate of neutron stars with $B_0\sim10^{15}$ G may be small compared to the total SN rate, $M_{\rm ej}^r$ may be large enough to account for the lower rate and accord with the total galactic r-process budget (see §1). That $M_{\rm ej}^r$ is not ejected isotropically may be important for the statistics of r-process enrichment in the early galaxy.

4. Some Open Questions

Trapping Timescale: Equations (1) and (2) are only applicable if $\tau_{\rm trap}$ is much shorter than all other timescales in the problem. We expect global wind quantities to change on the timescale for neutrino diffusion and luminosity decay. For example, the $B_0 = 2\times10^{15}$ G line in Fig. 3 has $\tau_{\rm trap}\simeq 0.05$ s and $\Delta s\simeq 90$ for the highest L_ν shown (shortest $\tau_{\rm dyn}$). Because $\dot{q}$ and $\dot{M}$ do not change significantly over $\tau_{\rm trap}$, we expect the result presented in Fig. 3 to be relatively robust. However, taking the $B_0 = 6\times10^{14}$ G line in Fig. 3, for the lowest L_ν (longest $\tau_{\rm dyn}$), we find that $\tau_{\rm trap}\simeq 11$ s and $\Delta s\simeq 650$. In this case $\tau_{\rm trap}$ is nearly as long as the cooling/wind epoch itself and the approximations of this paper break down.

Complex Field Topologies: The magnetic field may be a complex of higher order multipoles with a variety of local field strengths in this very early phase of PNS evolution. In this case we may consider a distribution of closed loops on the PNS surface. Qualitatively, this should not alter the conclusions of this paper - there would simply be a distribution of $\tau_{\rm trap}$ and corresponding Δs locally. For $M_{\rm ej}^r$, we need only estimate the covering fraction of closed loops. Interestingly, such considerations lead one to consider magnetic reconnection as a possible energy deposition mechanism (QW). Naively, including such a term in $\dot{q}$ may increase the entropy of the affected matter. QW and TBM showed that $\sim 10\%$ increases to the total energy deposition rate can significantly increase $s_{\rm a}$, but that the radial position of an enhancement in $\dot{q}$ is paramount to determining whether or not the entropy is increased asymptotically in the flow.

MHD Instabilities: The estimate of Δs in eq. (2) relies on the stability of the closed region over a time $\tau_{\rm trap}$. Given the action of neutrino heating and the geometry of the closed zone, it is possible that MHD instabilities might disrupt the system. If the timescale for instabilities to grow is much shorter than $\tau_{\rm trap}$ *and* the instability allows for the rapid removal of matter from the closed zone, the entropy enhancements shown in Fig. 3 may be significantly decreased. Because of line-tying we expect global interchange instabilities to be suppressed (J. Arons, private communication). Ballooning modes at R_β may develop rapidly, but allow for only a small amount of matter to escape in $\tau_{\rm trap}$. Perhaps such instabilities are the only way to remove the high entropy matter interior to R_q (see §2). A detailed stability analysis, or the solution to the full time-dependent MHD problem is required.

Rotation & Convection: Similar to MHD instabilities, rapid differential rotation or convection may disrupt the global magnetic field configuration on timescales much shorter than $\tau_{\rm trap}$, and thereby compromise the entropy amplifications calculated here. Even the shortest significant $\tau_{\rm trap}$ calculated in Fig. 3 is 50 ms in duration, which may be much longer than the initial PNS rotation and convective overturn timescales (Duncan & Thompson 1992; Thompson & Duncan 1993).

Spindown: The wind itself may slow the PNS rotation, carrying away angular momentum as the PNS contracts and cools. The PNS spins down on a timescale $\tau_J = J/\dot{J} \sim (3/5)MR^2/\dot{M}R_\beta^2$ (e.g. Lamers & Cassinelli 1999; Weber & Davis 1967). Taking the 'Low L_ν' solution ($\dot{M} \sim 10^{-7}\,{\rm M_\odot\,s^{-1}}$) and $B_0 = 10^{16}\,$G, we find $R_\beta \sim 2000\,$km and $\tau_J \sim 200\,$s – too long in comparison with all other relevant timescales to influence the PNS period significantly. For constant R, we see that for $L_\nu \propto t^{-\alpha}$ and $R_\beta \propto L_\nu^{-0.75}$ that $\tau_J \propto t^\alpha$; the increase in R_β as L_ν decreases is insufficient to counter the rapidly decreasing mass flux. Of course, this neglects the coupling between B_0 and the rotation of the PNS, which likely exists if the magnetic field is generated by either a standard or turbulent/convective dynamo (Thompson & Duncan 1993; Thompson & Murray 2001). These estimates for τ_J, however, assume the definition for R_β in §2 and that $B \propto r^{-3}$. Modifications to these assumptions change τ_J significantly.

5. Summary, Conclusions, & Implications

For the first time, we consider the effect of a strong dipole magnetic field on protoneutron star winds and the resulting nucleosynthesis in their ejecta. We show that magnetar-like field strengths can dominate the wind dynamics at all times during the PNS cooling epoch (see Fig. 1). We argue that at radii close to the PNS, matter may be trapped by closed magnetic field lines where $\beta < 1$. The matter in any closed region is not trapped permanently, but escapes on a timescale $\tau_{\rm trap}$, as a result of neutrino heating and the necessarily commensurate increase in both pressure and entropy. As β approaches unity in the closed zone, the material escapes dynamically. In Fig. 3 we show that for surface magnetic field strengths $\gtrsim 6\times10^{14}$ G, the entropy enhancement engendered by this trapping effect is sufficient to yield robust, 3$^{\rm rd}$-peak r-process nucleosynthesis. In this way, the factor of $\sim 3-5$ in entropy previously unattained in spherical models of PNS winds may be achieved. That the r-process would occur at high entropy (and not, necessarily, at very short $\tau_{\rm dyn}$, as in TBM) in these models might help explain how, in the multi-dimensional parameter space of supernovae and PNS cooling, the same r-process abundance profile above $A \sim 135$ is observed in both the sun and ultra-metal-poor halo stars (see §1). A close look at the models of Meyer & Brown (1997) reveals that at $s_{\rm a} = 500$, for $\tau_{\rm dyn} \sim 0.06$, there is considerable leeway in choosing $Y_e^{\rm a}$ (say 0.48 to 0.42) so that, approximately, the relative r-process abundances for $135 \lesssim A \lesssim 195$ accord well with those from the sun. For a given $Y_e^{\rm a}$, similar flexibility in $\tau_{\rm dyn}$ also exists at high $s_{\rm a}$ (also implied by results of Otsuki et al. 2002).

Clearly, much more work is required to understand wind emergence, evolution, and nucleosynthesis during the cooling epoch of highly magnetized protoneutron stars. This preliminary investigation is merely the first step in quantifying one of the panoply of possible effects. Although the magnitude of the entropy enhancement caused by trapping in closed magnetic loops is indicated in Fig. 3, detailed numbers and systematics must await multi-dimensional MHD models. That said, however, we here forward the idea that neutrino-driven winds from nascent protoneutron stars with magnetar-like surface field strengths are responsible for the production of the heavy r-process nuclides we find in nature.

The author is indebted to Jon Arons, Eliot Quataert, and Adam Burrows for a critical reading of the text and to Anatoly Spitkovsky, Stan Woosley, Lars Bildsten, and Henk Spruit for helpful conversations. Insightful comments and suggestions for improvement of the manuscript by the referee, Al Cameron, are also acknowledged. Support for this work was provided by NASA through Hubble Fellowship grant #HST-HF-01157.01-A awarded by the Space Telescope Science Institute, which is operated by the Association of Universities for Research in Astronomy, Inc., for NASA, under contract NAS 5-26555.

REFERENCES

[1]Burbidge, E., Burbidge, G., Fowler, W., & Hoyle, F. 1957, Rev. Mod. Phys., 29, 547

[2]Burris, D. L., Pilachowski, C. A., Armandroff, T. E., Sneden, C., Cowan, J. J., & Roe, H. 2000, ApJ, 544, 302

[3]Burrows, A., Hayes, J., & Fryxell, B. A. 1995, ApJ, 450, 830

[4]Cameron, A. G. W. 1957, PASP, 69, 201

[5]Duncan, R. C. & Thompson, C. 1992, ApJ, 392, L9

[6]Hoffman, R. D., Woosely, S. E., & Qian,Y.-Z. 1997, ApJ, 482, 951

[7]Kouveliotou, C. et al. 1999, ApJ, 510, L115

[8]Lamers, H. & Cassinelli, J. P., *Introduction to Stellar Winds* (Cambridge University Press, Cambridge, 1999)

[9]Lionello, R., Linker, J. A., & Mikíc, Z. 2001, ApJ, 546, 542

[10]Mestel, L. 1968, MNRAS, 138, 359

[11]Meyer, B. S. & Brown, J. S. 1997, ApJS, 112, 199

[12]Nagataki, S. & Kohri, K. 2001, PASJ, 53, 547

[13]Otsuki, K., Tagoshi, H., Kajino, T., & Wanajo, S.-Y. 2000, ApJ, 533, 424

[14]Otsuki, K., Mathews, G., & Kajino, T. 2002, astro-ph/0207596

[Pneuman & Kopp]Pneuman, G. W. & Kopp, R. A. 1971, 18, 258

[15]Qian, Y.-Z. 2000, ApJ, 534, L67

[16]Qian, Y.-Z. & Woosley, S. E. 1996, ApJ, 471, 331 (QW)

[17]Sneden, C., McWilliam, A., Preston, G. W., Cowan, J. J., Burris, D. L., & Armosky, B. J. 1996, ApJ, 467, 819

[18]Steinolfson, R. S., Suess, S. T., & Wu, S. T. 1982, ApJ, 255, 730

[19]Takahashi, K., Witti, J., & Janka, H.-T. 1994, A&A, 286, 857

[20]Terasawa, M., Sumiyoshi, K., Yamada, S., Suzuki, H., Kajino, T. 2002, ApJ, 578, L137

[21]Thompson, T. A., Burrows, A., & Meyer, B. S. 2001, ApJ, 562, 887 (TBM)

[22]Thompson, C. & Duncan, R. C. 1993, ApJ, 408, 194

[23]Thompson, C. & Murray, N. 2001, ApJ, 560, 339

[24]Usmanov, A., Goldstein, M., Besser, B., & Fritzer, J. 2000, J. Geophys. Res., 105, 12675

[25]Wanajo, S., Kajino, T., Mathews, G. J., & Otsuki, K. 2001, ApJ, 554, 578

[26]Weber, E. J. & Davis, L. 1967, ApJ, 148, 217

[27]Woosley, S. E. & Hoffman, R. D. 1992, ApJ, 395, 202

[28]Woosley, S., Wilson, J., Mathews G., Hoffman, R., & Meyer, B. 1994, ApJ, 433, 209

Fig. 1.— Two representative wind pressure profiles (solid lines, $\log_{10}[\mathrm{erg\,cm^{-3}}]$) as a function of radius for 'High' and 'Low' neutrino luminosity (L_ν) for a neutron star with gravitational mass $1.4\,\mathrm{M}_\odot$ and coordinate radius $R_\nu = 10\,\mathrm{km}$. Also shown are profiles of magnetic energy density ($\log_{10}[B^2/8\pi\ (\mathrm{erg\,cm^{-3}})]$, dashed lines) assuming $B = B_0(R_B/r)^3$, where the reference radius $R_B = 11\,\mathrm{km}$, for surface magnetic field strengths of 10^{13}, 10^{14}, 10^{15}, and 10^{16} G.

Fig. 2.— T (MeV), s, and ρ ($\log_{10}[\mathrm{g\ cm^{-3}}]$), for the 'High L_ν' wind solution (thin solid lines, compare with Fig. 1). For given $\rho(r)$, dotted lines show $T^*(r)$ and $s^*(r)$, the maximum temperature and corresponding entropy that can be attained before cooling balances neutrino heating (see §2). For $B_0 = 5\times10^{15}$ G, the thick solid line shows $s+\Delta s$, where Δs is computed using eq. (2). For this wind model and assumed B_0, $R_q \simeq 23\,\mathrm{km}$ and $R_\beta \simeq 125$.

Fig. 3.— Asymptotic entropy (s_a) versus dynamical timescale (τ_dyn) for a collection of PNS wind models with $R = 10\,\mathrm{km}$ and $M = 1.4\,\mathrm{M}_\odot$ as a function of neutrino luminosity (L_ν). The thick solid line shows the evolution of the wind solutions in the s_a-τ_dyn plane without including any magnetic field effects. Thin solid lines show the same curve, but including the amplification in s_a due to $B_0 = 2\times10^{14}$, 4×10^{14}, 6×10^{14}, 8×10^{14}, 1×10^{15}, and 2×10^{15} G as per eq. (2). The heavy dashed line shows, for $Y_e^\mathrm{a} = 0.48$, the line in the s_a-τ_dyn plane above which 3$^\mathrm{rd}$-peak r-process nucleosynthesis is likely (from Hoffman, Woosley, & Qian 1997).

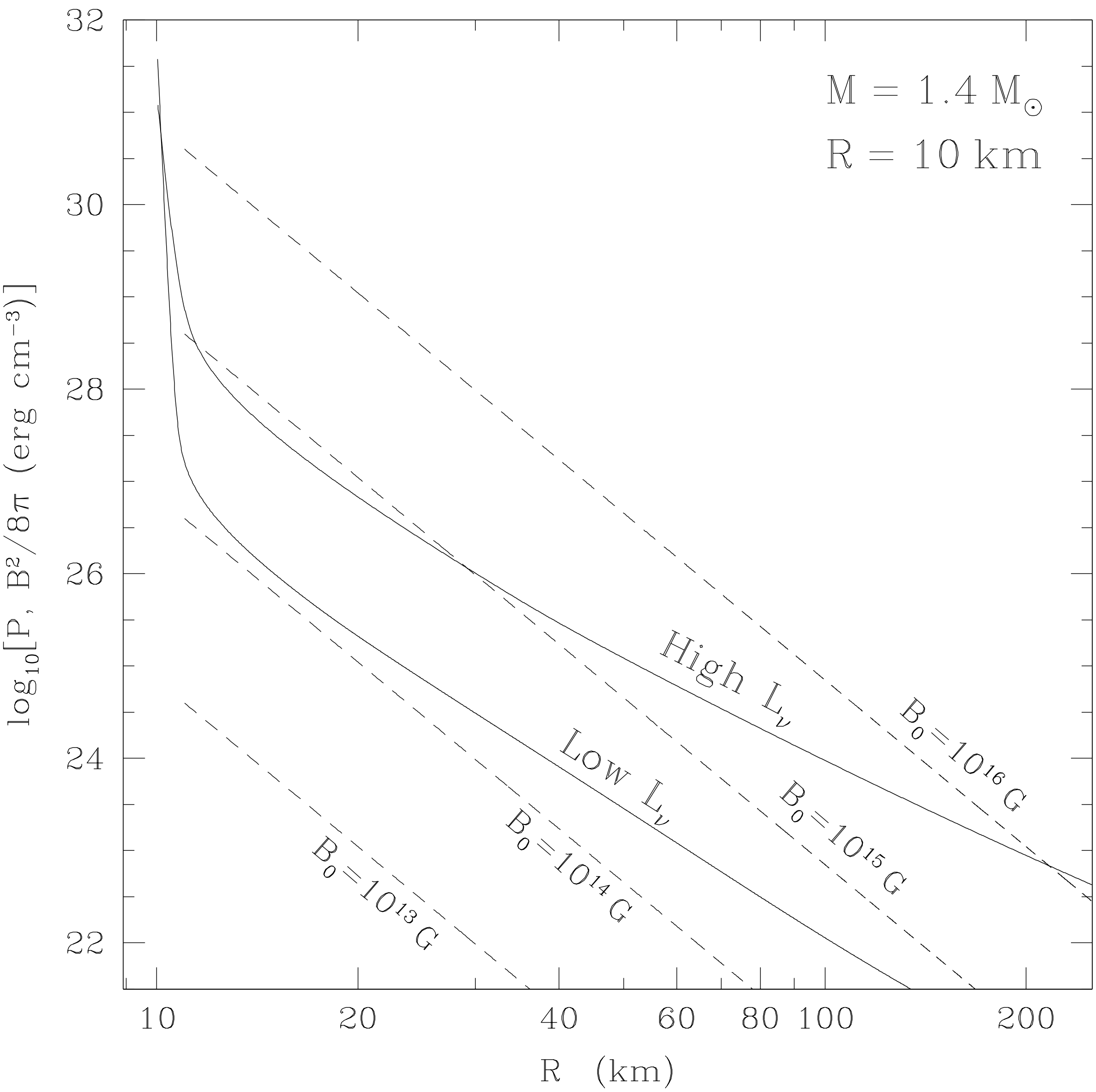
M = 1.4 $M_\odot$
R = 10 km
High L_ν
Low L_ν
$B_0 = 10^{16}$ G
$B_0 = 10^{15}$ G
$B_0 = 10^{14}$ G
$B_0 = 10^{13}$ G
$\log_{10}[P,\ B^2/8\pi\ (\mathrm{erg\ cm^{-3}})]$
R (km)
32
30
28
26
24
22
10
20
40
60
80
100
200

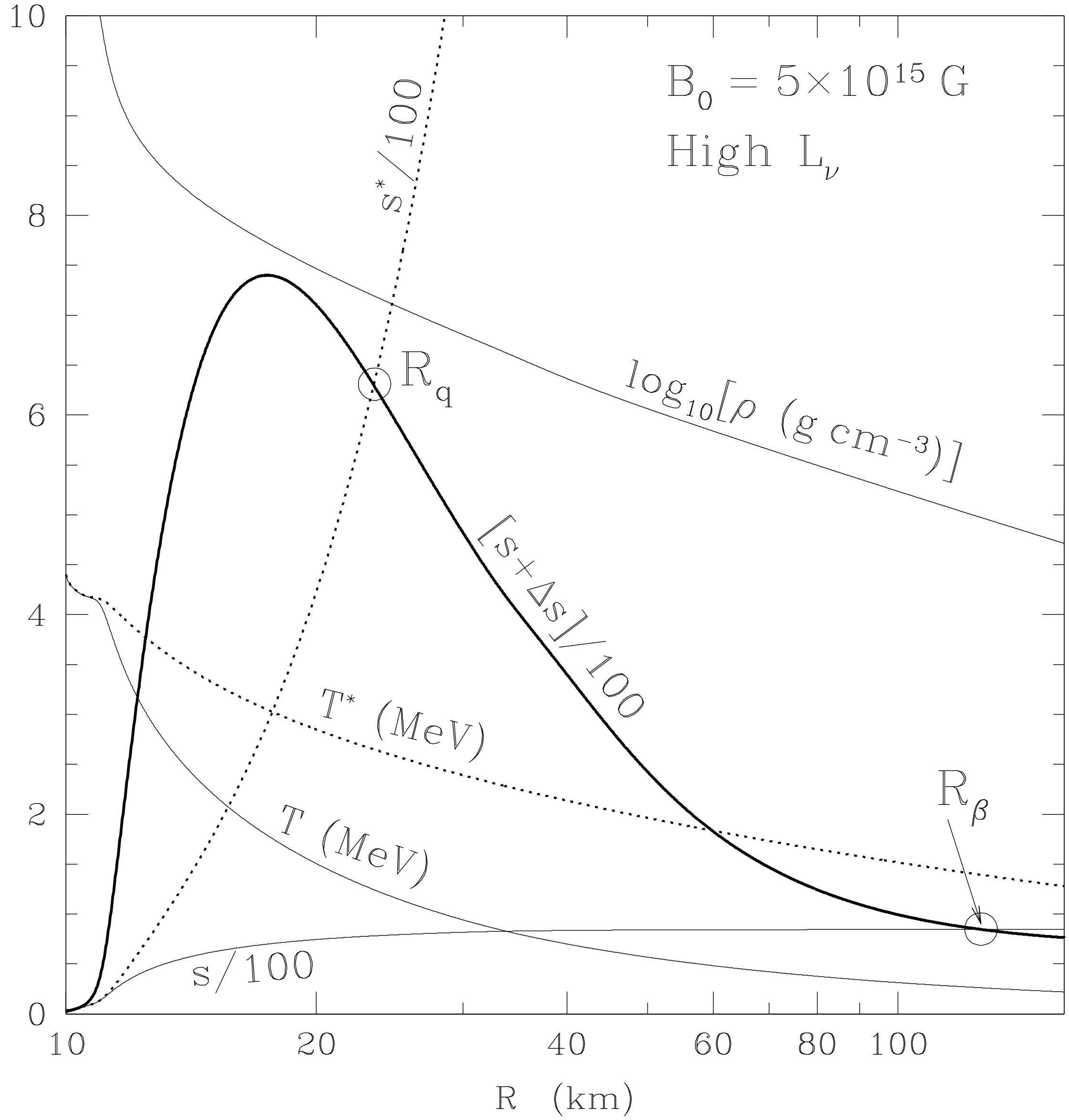

$B_0 = 5\times10^{15}$ G
High L_ν
$s^*/100$
R_q
$\log_{10}[\rho$ (g cm^{-3})]
$[s+\Delta s]/100$
T^* (MeV)
T (MeV)
R_β
s/100
R (km)

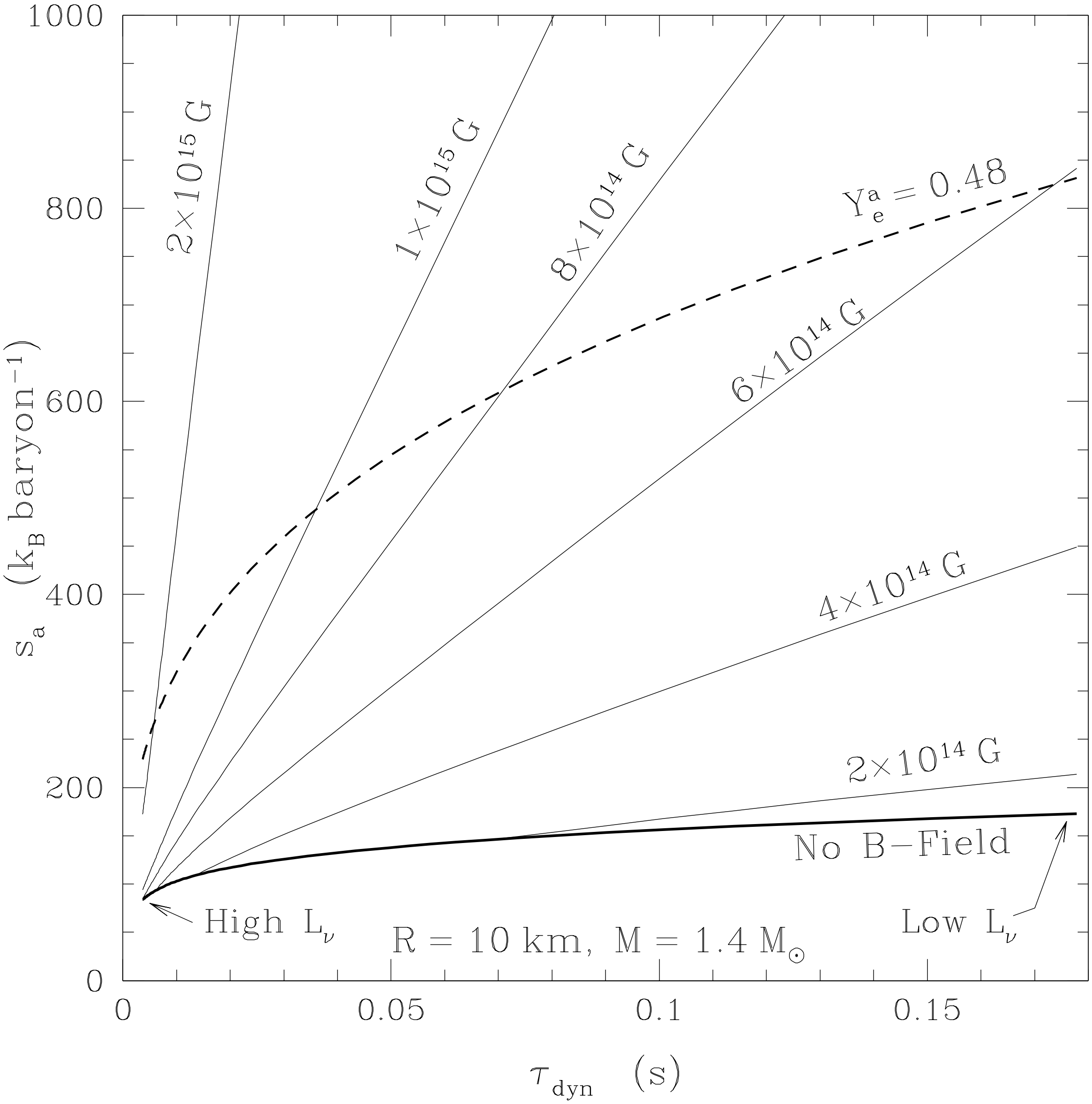
1000
800
600
400
200
0
0
0.05
0.1
0.15
s_a (k_B baryon^{-1})
τ_{dyn} (s)
2×10^{15} G
1×10^{15} G
8×10^{14} G
$Y_e^a = 0.48$
6×10^{14} G
4×10^{14} G
2×10^{14} G
No B–Field
High L_ν
$R = 10$ km, $M = 1.4\ M_\odot$
Low L_ν